https://doi.org/10.1016/j.energy.2018.11.073

Investigation into spacing restriction and layout optimization of wind farm with multiple types of wind turbines

Haiying Sun[a], Hongxing Yang[a]*, Xiaoxia Gao[b]

[a]Renewable Energy Research Group, Department of Building Services Engineering, The Hong Kong Polytechnic University, Hong Kong
[b]Department of Power Engineering, North China Electric Power University (Baoding), Baoding, PR China

Abstract

In this paper, a new Directional Restriction method is presented to restrict the spacing between wind turbines. Compared to existing restrictions, the new method additionally considers the influence of wind directions, and the restriction for each wind turbine is related to its rotor diameter. Therefore, the method is especially effective for the site with obvious prevailing wind directions. With the Directional Restriction, a wind farm optimization process applying the Multi-Population Genetic Algorithm has been presented. The optimization can exploit the wind resource more effectively and can be used to optimize the layout of nonuniform wind farm. Four representative cases are then studied and discussed: (a) aligned layout with uniform wind turbines; (b) optimized layout with uniform wind turbines; (c) optimized layout with nonuniform wind turbines and (d) a commercial nonuniform offshore wind farm. Through these cases, the utilization rate of a nonuniform wind farm with five types of wind turbines can increase to 99.21%, in which the minimum utilization rate of a single wind turbine is 94.27%. Especially, in the last case, a potential offshore wind farm in Sha Chau Island in Hong Kong is analyzed. The results demonstrate that the proposed optimization method is practical in designing wind farms. The coastal area in Hong Kong is the ideal region to develop offshore wind power.

Keywords: The Directional Restriction; Wind farm layout optimization; Multiple types of wind turbines; Wake effect.

1. Introduction

Energy demand is an important input for socio-economic development, and it tends to increase dramatically with the annual increase of the global population and economy [1]. Among various types of energy, renewable energy is the most prospective one as for its inexhaustible characteristic. In addition, renewable energy is clean and environment-friendly, therefore it is the ideal energy source to resist the increasing global warming and pollution problems.

Wind power, a typical renewable energy, is developing rapidly nowadays. Annual installation of the global wind industry was 52.492 GW at the end of 2017, which added the new global total to 539.123 GW, and this growth was in large part powered by 19.66 GW new installations figure in China [2]. Especially, compared with onshore wind resources, their counterpart offshore wind resources tend to be abundant, stronger, and more consistent in terms of their availability [3]. The offshore wind also has a higher efficiency in energy production, saves more land area [4] and has less impact on residents [5]. As expected, offshore wind power is more and more becoming a major source of energy globally and is already a major development in electricity generation for many marine countries [6]. In the year 2017, there was 18.81 GW offshore wind power capacity in 17 markets around the world [2]. Nearly 84% (15.78 GW) was located in offshore waters of 11 European countries. The remaining 16% was located mainly in China, followed by Vietnam, Japan, South Korea and the United States [2]. However, the most noteworthy thing is that the 13th Five-Year Plan of China sets a target of 5 GW offshore wind industry to be installed in China by 2020, which may change that pattern.

Corresponding author. Tel.: 2766 5863
E-mail address: hong-xing.yang@polyu.edu.hk

Hong Kong is also an ideal coastal region to make use of offshore wind energy, with an annual power generation potential of 1.13×10^{10} kWh [7], accounting for 25.54% of the total annual electricity consumption in 2014 [8]. However, the energy in Hong Kong now is either imported directly (oil products and coal products), or produced using imported fuel inputs (nuclear electricity and gas), only excluding a very small scale of wind power generation as from early 2006 [9], and with no energy supplement from the offshore wind yet. It is reported that around 90% of the total greenhouse gas emissions (44,400 kilotons CO2) originated from the consumption of energy [8]. Therefore, Hong Kong stands a good chance to develop the offshore wind energy industry in the near future.

When designing a wind farm, a spacing restriction must be set to minimize the influence of wake effect on a wind turbine (WT) and the WTs' interaction effect. The most common methods are the wind farm grid method and the Omnidirectional Restriction. The wind farm grid method sets the same-size cells in a wind farm and installs WTs in the center of cells. Omnidirectional Restriction method is to set a minimum distance restriction around all WTs, and five times of the rotor diameter is widely used. These two methods actually both excessively restrain the crosswind intervals between WTs, because the wake develops in downwind direction and the WTs in crosswind direction are hardly influenced by the wake effect. Thus, if these methods are adopted, huge space will be wasted, especially where the directions of prevailing wind are strongly centralized. On the other hand, with the experience in wind industry is accumulated, it is a trend to develop the nonuniform wind farm, which involves multiple types of WTs. So far, few studies have been conducted on how to set restrictions among various types of WTs. One rough way is to make sure that the distance between two WTs is at least five times of the larger WT's rotor diameter [10]. It is easily concluded that this limitation is just an extension of the Omnidirectional Restriction, which causes the spacing waste in the nonuniform wind farm. Therefore, some more studies should be conducted to make good use of the space in wind farms, and a new feasible spacing restriction that considers the influence of wind direction is needed.

This study presents a new directional spacing restriction method and investigates the wind farm layout optimization problem. In section 2, the current spacing restrictions in wind farm optimizations are introduced and a new Directional Restriction is presented. The new method separately limits the interval between WTs in downwind and crosswind directions, which tends to make better use of wind resources. In section 3, a comprehensive literature review on nonuniform wind farm optimization problems is conducted. Limitations and development prospects are analyzed. In section 4, the WT models, the wind farm model and the wake model used in this study are introduced in detail. In section 5, four typical cases are demonstrated to show the effectiveness of the new Directional Restriction and the nonuniform wind farm optimization method. A commercial offshore wind farm design in Hong Kong is also involved, which is a practical guide for the development of wind industry in Hong Kong. In section 6, main conclusions of this study are drawn. The achievement of this research will contribute to the nonuniform wind farm optimization, especially for the wind field with centralized prevailing wind directions.

Nomenclature

a	axial induction factor	u	incoming wind velocity of the downstream WT (m/s)
Δd	horizontal distance of WTs perpendicular to the downstream direction (m)	v_0	known wind speed at z_0 (m/s)
Δh	hub height difference between two WTs (m)	v	wind speed at height of z (m/s)
s_0	swept area of the WT (m^2)	V_g	gradient wind velocity (m/s)
s_w	wake area of the downstream WT (m^2)	x	distance between the upstream and the downstream WTs (m)
r_0	rotor radius of the WT (m)	z_0	reference height (m)
r_w	radius of the wake area (m)	α	wind speed power law parameter
u_0	incoming wind velocity at z_0 height (m/s)	δ	boundary-layer thickness (m)

2. Spacing restrictions in wind farm optimization

In a wind farm, a WT must be installed at a distance from other WTs. One practical consideration is to avoid the huge influence of wind deficits and turbulence from the upwind WTs, and the other one is to prevent the interaction effect among WTs. Consequently, a restriction must be set when designing and optimizing a wind farm.

In the earlier research on the wind farm layout optimization problems, a grid farm was always applied to restrain the position of WTs, as shown in Figure 1. Mosetti, et al. [11] used a 10×10 square grid farm to solve wind farm optimization problems. The size of each cell was 5D (D represents the rotor diameter of the wind turbine) and WTs must be placed at the midpoints of the square cells. Grady, et al. [12] further studied the wake decay effect in wind farm design with Genetic Algorithm, using the same wind farm grid. Zhang, et al. [13] applied a lazy greedy algorithm to optimize the placement of WTs, in which a 10×10 square grid farm with 5D side length was also used.

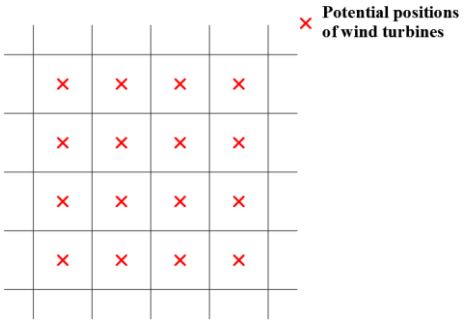

Figure 1 Wind farm grid with potential positions of wind turbines

Recently, the more general way is to set a minimum distance between any two WTs, which is the empirical Omnidirectional Restriction. It can be interpreted by a circular restrained area, and 5D restrained radius is mostly used, as shown in Figure 2. In the Omnidirectional Restriction, each WT has its restrained area, and any other WTs should not be installed in it. If one WT (WT2) is put into the restrained area of another WT (WT1), both two WTs (WT1 and WT2) are regarded as out of operation, which means their power outputs are considered as zeros. This restriction is widely used in optimizing the layout of wind farms because of its simplicity.

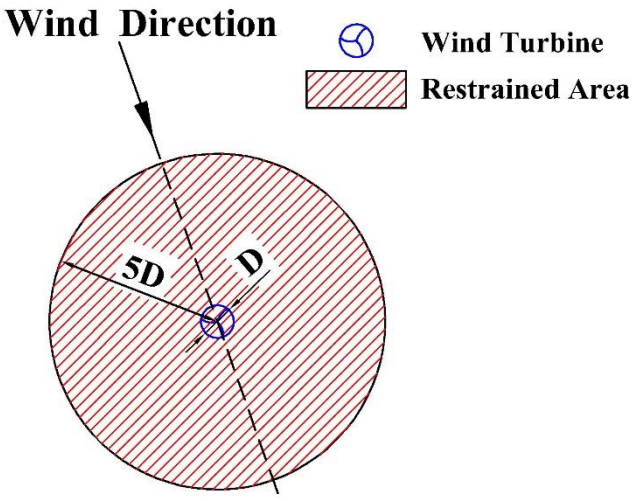

Figure 2 Restrained area in the Omnidirectional Restriction.

Park and Law [14] described a method for optimizing the placement of WTs with the 5D inter distance constraint. Mittal, et al. [15] proposed a hybrid optimization method to simultaneously optimize the total number and the locations of WTs, in which the minimum distance between WTs is 5D. Parada, et al. [16] also determined the wind farm layout to maximize the annual energy generated, using the Omnidirectional Restriction with the 5D constraint.

The Omnidirectional Restriction is more advanced than the wind farm grid restriction. However, the irrationality of it is obvious. The wake generates behind the WT blades and then develops in the wind direction. For a specific wind direction, the wake influenced area is within a long downwind distance but a relatively short crosswind distance. The Omnidirectional Restriction does not consider the directional influence from the wake effect. For the place where the prevailing wind directions are very distinct, it is especially not economical when adopting the Omnidirectional Restriction to design a wind farm.

Actually, in real projects, some representative wind farms do not adopt the traditional Omnidirectional Restriction, because the local wind conditions are special. Tehachapi Pass Wind Farm [17], as shown in Figure 3, is a large-scale wind farm installed in the early year in the United States. The local prevailing wind direction is highly-centralized. Corresponding to the wind condition, its layout is also characteristic, with the very small crosswind intervals between WTs (some are even less than 1.5D) and the much larger downwind intervals (some are larger than 5D). This layout makes a better use of the wind resource, and the parallel installed WTs have little influence on each other as well.

Figure 3 Aerial view of the Tehachapi Pass Wind Farm [17]

Therefore, inspired by the Tehachapi Pass Wind Farm, a new Directional Restriction is presented in this paper, as shown in Figure 4. The Directional Restriction tends to make good use of wind resources, save the occupied area of a wind farm and decrease the cost of energy. When adopting the Directional Restriction, the restrained area varies with the wind direction. For a particular wind direction, the restrained distance in the downwind direction is 5D, and that distance in the crosswind direction is much smaller, 3D is set in this study. It can be seen that the restrained area of the new Directional Restriction is much smaller than that of the Omnidirectional Restriction. The application of the Directional Restriction in layout optimization is also different from the Omnidirectional Restriction. When adopting the Directional Restriction, as shown in Figure 4, if one WT (WT2) is put into the restrained area of another WT (WT1), only WT2 is regarded as out of work, whereas WT1 is still assumed to work normally. This assumption is much closer to the reality compared to the Omnidirectional Restriction.

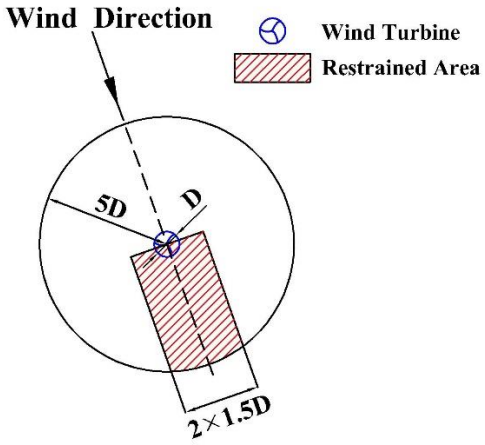

Figure 4 Restrained area in the Directional Restriction.

So far, no research has been conducted on the Directional Restriction or other wind direction

dominant restrictions. This study tries to fill in this research gap. In this paper, the newly presented Directional Restriction is applied to both aligned and optimized wind farm layouts. The advantages and the feasibilities are studied and discussed from the aspect of energy output. This study is of value to the wind farm development in the region where the wind is highly-concentrated.

3. Nonuniform wind farm optimization

The Directional Restriction also contributes to the layout optimization of nonuniform wind farms, which contain different types of WTs. Since the nonuniform wind farms increase the difficulties in optimization, for a long time, studies were only carried out based on the one-type-WT wind farm. However, some recent research has found that the nonuniform wind farm may be a better choice.

Herbert-Acero, et al. [18] addressed the problem of WTs lined up in the wind direction through three cases, in which the simulated annealing [19] and genetic algorithms [20] were used. From the result, their algorithms can minimize wake effects by placing the WT hubs at two different heights. Chen, et al. [21] used a nested genetic algorithm to analyze different hub heights' effect on energy output in a small onshore wind farm. The results showed that the energy output can increase by using WTs with various hub heights when the total number of WTs is same. Chowdhury, et al. [22] developed an optimization for the commercial-scale wind fields to decide the type and the position of WT to install. The Particle Swarm Optimization algorithm was used. From their results, the capacity factor of wind farm increased to a noteworthy 6.4% when optimizing the position and the type of WT simultaneously. Chen, et al. [23] firstly conducted the research on WT height matching problem in wind farm layout optimization. The greedy algorithm was used and the optimal objective was to find the maximum Turbine-Site Matching Index, including cost and production of the wind field. The presented iteration method was then validated through both numerical cases of both flat terrain and complex terrain. Then they continued the study of the multiple WT height optimization with the greedy algorithm [24]. A three-dimensional greedy algorithm was built to optimize the wind farm with various WT hub heights and reduce the cost of energy. The layout of wind farm with different hub heights increased the total energy output and reduced the cost of energy compared to that with identical hub heights, especially for the wind field in the complex terrain. Lee, et al. [25] proposed a hub height optimization method with the objective of Annual Net Profit, which provided the economic feasibility of WTs. The optimal hub height reduced with the increase of the wind shear exponent and the mean wind speed. Of all WT power characteristics, the optimal WT hub height was mostly affected by the rated speed and the cut-out speed. Feng and Shen [10] investigated the nonuniform offshore wind farms layout design with both different types of WTs and WT hub heights. They built a random search algorithm and it was validated through the Horns Rev 1 offshore wind farm. The difference between the optimal nonuniform designs and their uniform counterparts was that the nonuniform one achieved a better economical performance, as per MW of the smaller size turbine needs less investment. Vasel-Be-Hagh and Archer [26] assessed the effect of only one optimal variable, the WT hub height, on the Annual Energy Production of a wind field. Three cases were discussed and then the findings were validated by the large eddy simulations. Song, et al. [27] investigated the WT layout optimization of different hub heights on flat terrain with the Gaussian Particle Swarm Optimization. All WT positions and the WT hub heights were optimized simultaneously. Then they drew the conclusion that their method can produce optimum solutions with relatively high energy output and low cost per unit product in most circumstances, which is more obvious in some complicated situations.

To sum up, the investigation on nonuniform wind farm optimization is developing but still not comprehensive at the present stage. Among the limited research, most of them [18, 21, 23-27] just consider the hub height as the variable, and only two [10, 22] adopt different types of WTs. To be specific, references [18, 21, 24, 26] involve two alternative hub heights, and references [23, 25, 27] consider a series of hub heights within the designated height arrangement. As for the multiple WTs studies, the reference [10] involves three different types of WTs, of which each type of WT has a hub height; whereas the reference [22] studies three types of WTs but with five hub heights. Through these studies, it can be analyzed that if diverse WTs are involved, not only the wind speed at different heights need to be considered, the factors such as the wake influenced space, wake induced energy losses and restrictions between different WTs should not be ignored as well. So far, most nonuniform optimization studies are restricted to the WT hub height optimization, which simplifies the problems, which apparently should be investigated more extensively and deeply. Therefore, in this paper, the nonuniform wind farm optimization is not limited to the hub height optimization, but also contains different types of WTs. The adopted WTs have differing characteristics in hub heights, rotor radius, rated power and rated wind speed, etc. The specification of the WTs is demonstrated in section 4.2.

4. Calculation models

In this chapter, the crucial models used in this study are introduced, including WT models, the wind farm model and the wake model.

4.1 Wind turbine models

To investigate the wind farm optimization problem with multiple types of WTs, five differing types of WTs are adopted in this study. The WTs are chosen from ENERCON products [28], and the five types are E-126, E-126 EP4, E-101, E-82 and E-44. The rated powers range from 900 kW to 7580 kW, and the service time is assumed to be 20 years for each WT. The key parameters of WTs are listed in Table 1. It is clear that not only the hub heights are diverse, but the rotor diameters, cut-in speeds and rated speeds are different as well.

Table 1 The parameters of wind turbines [28]

Parameters	E-126	E-126 EP4	E-101	E-82	E-44
Rated power (kW)	7580	4200	3050	2000	900
Rotor diameter (m)	127	127	101	82	44
Cut-in speed (m/s)	3	3	2	2	3
Rated speed (m/s)	17	14	13	13	17
Cut-off speed (m/s)	25	25	25	25	25
Hub height (m)	135	135	99	78	45
Service years	20	20	20	20	20

In this study, the power curves of WTs are utilized to estimate the wind farm's output. Figure 5 and Figure 6 demonstrate the power curves and the power coefficient curves of the five chosen WTs respectively [28].

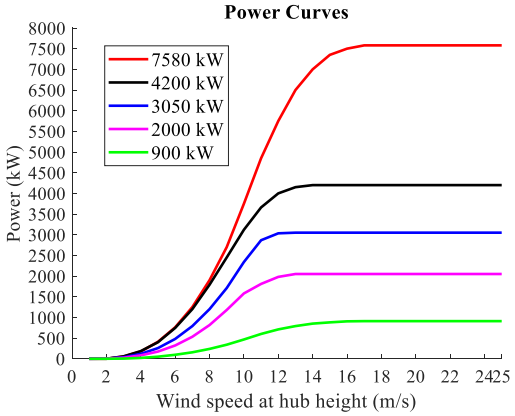

Figure 5 Power curves of the chosen wind turbines

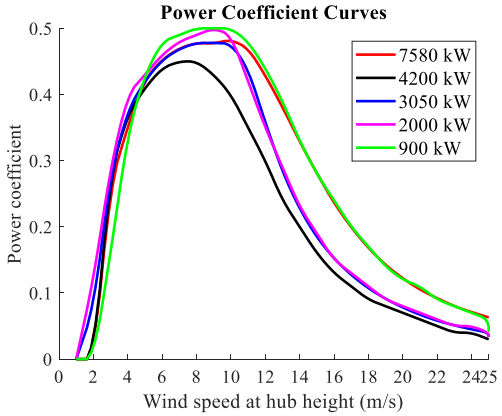

Figure 6 Power coefficient curves of the chosen wind turbines

4.2 Wind farm model

The wind farm model is built based on matrixes. The position of WT is expressed by coordinate, and the relative position of any two WTs is expressed by the vector with magnitude and direction. The wind loads are represented by vectors correspondingly, of which the magnitude and direction represent the wind speed and the wind direction, respectively. The diagram of the matrix expression of the distance between WTs in wind direction is shown in Figure 7.

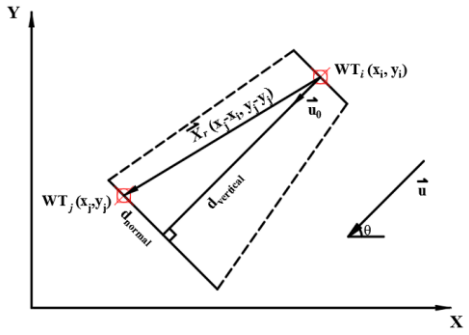

Figure 7 Distance between turbines in wind direction

From the figure, X axis and Y axis are the wind farm's coordinate axes. The red points WT_i and WT_j on the diagram represent two WTs in the wind farm. (x_i, y_i) and (x_j, y_j) are the position coordinates of WT_i and WT_j, respectively. $\vec{X}_r$ is the vector from WT_i to WT_j, which can be calculated from the equation $\vec{X}_r = (x_j - x_i, y_j - y_i)$. $\vec{u}$ is the wind velocity vector, obtained from the input wind data. Then, $\vec{u}_0$, the unit vector of $\vec{u}$, can be calculated from $\vec{u}_0 = \frac{\vec{u}}{\|\vec{u}\|}$. d_{normal} and $d_{vertical}$ can be obtained from $\vec{X}_r$ and $\vec{u}_0$ through the vector calculation, the equations are listed as follows:

$$d_{normal} = \vec{X}_r \cdot \vec{u}_0 \tag{1}$$

$$d_{vertical} = \vec{X}_r \times \vec{u}_0 \tag{2}$$

From Figure 7, d_{normal} and $d_{vertical}$ are two important parameters to account the wake effect. $d_{vertical}$ is to judge the relative position of two WTs: if $d_{vertical}$ is positive, WT_i is the upstream WT and WT_j is the downstream WT, whereas if $d_{vertical}$ is minus, WT_i is the downstream WT and WT_j is the upstream WT. d_{normal} is to judge whether WT is under the wake's effect. When $|d_{normal}|$ is less than the wake radius of the upstream WT, the downstream WT is under the wake influence of the upstream WT, and then $d_{vertical}$ should be used to calculate wind losses according to the appropriate wake model.

In the MATLAB program, to keep calculation simple, WT position coordinates and relative position coordinates are extended from vectors to matrixes. If a wind farm with two WTs is considered, the position matrix $\vec{X}$ and relative position matrix $\vec{X}_r$ are as follows:

$$\vec{X} = \begin{bmatrix} (x_1, y_1) & (x_2, y_2) \\ (x_1, y_1) & (x_2, y_2) \end{bmatrix} \tag{3}$$

$$\vec{X}_r = \vec{X}' - \vec{X} = \begin{bmatrix} (x_1 - x_1, y_1 - y_1) & (x_1 - x_2, y_1 - y_2) \\ (x_2 - x_1, y_2 - y_1) & (x_2 - x_2, y_2 - y_2) \end{bmatrix} \tag{4}$$

For $\vec{X}_r$, the diagonal elements should not be involved in calculations, as no WT is under the wake

effect of its own. Correspondingly, when adopting equation (1) and equation (2), $\vec{X}_r$ should adopt equation (4) either.

In a real wind farm with multiple WTs, the wake-influenced situation of a WT may be complicated. For example, in Figure 8, the blue WT is under the wake effect of three red WTs, whereas the black one is under no-wake effect. So the calculation model based on multiple WTs should be further developed.

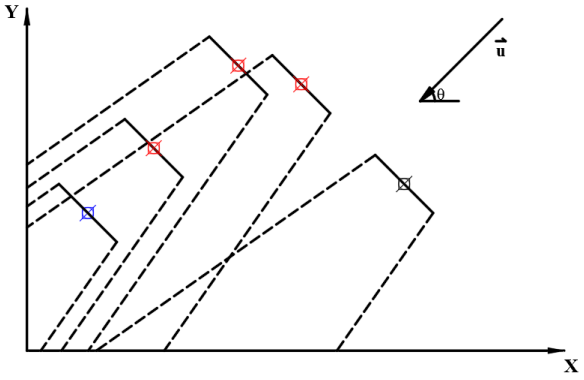

Figure 8 The wind turbines under wake effect

To build a calculation model of the whole wind farm, a complete position matrix is necessary. The position matrix $\vec{X}$ is extended from a two-dimensional (2-D) matrix to a multi-dimensional matrix, and correspondingly, $\vec{X}_r$ is also extended. Supposing the number of the WTs is N, $\vec{X}$ and $\vec{X}_r$ are expressed as follows:

$$\vec{X} = \begin{bmatrix} (x_1, y_1) & (x_2, y_2) & \text{K} & (x_N, y_N) \\ (x_1, y_1) & (x_2, y_2) & \text{K} & (x_N, y_N) \\ \text{M} & \text{M} & \text{O} & \text{M} \\ (x_1, y_1) & (x_2, y_2) & \text{K} & (x_N, y_N) \end{bmatrix} \tag{5}$$

$$\vec{X}_r = \vec{X}' - \vec{X} = \begin{bmatrix} (x_1 - x_1, y_1 - y_1) & (x_1 - x_2, y_1 - y_2) & \text{K} & (x_1 - x_N, y_1 - y_N) \\ (x_2 - x_1, y_2 - y_1) & (x_2 - x_2, y_2 - y_2) & \text{K} & (x_2 - x_N, y_2 - y_N) \\ \text{M} & \text{M} & \text{O} & \text{M} \\ (x_N - x_1, y_N - y_1) & (x_N - x_2, y_N - y_2) & \text{K} & (x_N - x_N, y_N - y_N) \end{bmatrix} \tag{6}$$

With the multi-dimensional matrix $\vec{X}_r$, the matrixes of d_{normal} and $d_{vertical}$ can be easily calculated as well. Then, the judgment of the wake effect of all WTs within a wind farm can be obtained accordingly.

4.3 Wake model

The wake affects the energy output efficiency of a wind farm seriously. The reason is that WT generates energy and induces wakes behind its swept areas simultaneously, and wakes will degrade the energy output performance of the downwind WT to a great extent [29]. In large wind farms, the power losses caused by wakes are 10-20% of the total power output [30, 31]. When designing a wind farm, taking the wake effect into consideration is an essential way to avoid much power losses. However, since the wake effect is complicated, its characteristics are still not veiled totally. Analytical wake models are the most commonly used measure to estimate wind losses when optimizing the layout of a wind farm. Analytical wake models are relevantly simple and are likely to meet the demands of both desired computation time and necessary accuracy of prediction. Several people have proposed wake models including, Jensen, Ainslie and G.C. Larsen [32]. All these models can be used in energy yields estimation, however, only Jensen wake model has been used in most wind farm layout design work [33-37].

Jensen wake model [38] (also known as Park model) is the most common choice to estimate the energy losses in wind farm due to its simplicity and relatively high accuracy. The calculation based on

Jensen wake model requires the least computation time compared with other models [39]. Jensen wake model is based on momentum conservation theory, and it assumes a linear wake expansion behind the upwind WT [38], as shown in Figure 9.

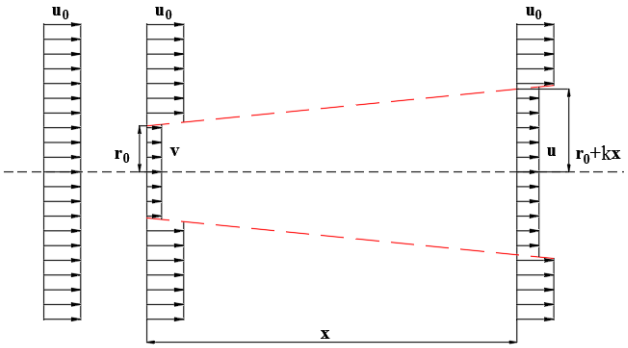

Figure 9 Jensen wake model

The equation of Jensen wake model is shown as equation (7) and equation (8). If a WT is under one WT's wake influence, equation (7) should be adopted; whereas if a WT is under several WTs' wake influence, a more complicated equation (8) should be used additionally.

$$u = u_0\left[1-\frac{2ar_0^2}{(r_0+kx)^2}\right] \tag{7}$$

$$u_i = u_0\left[1-\sqrt{\sum_{i=1}^{N}\left(1-\frac{u}{u_0}\right)^2}\right] \tag{8}$$

u_0 is the original wind velocity; r_0 is the radius of WT; a is the axial induction factor; x is the distance between the upstream WT and the downstream WT; and u is the incoming wind velocity of the downstream WT.

Although Jensen wake model is widely accepted, one apparent problem is that the wind velocity distribution behind the WT blades is not one-dimensional in reality. Assuming wake effect as a linear problem is far from reality. On the other hand, the three-dimensional (3-D) wake model can predict wind velocity precisely [40], but it is still too complicated to solve wind farm optimization problems. Thus in this study, a conceptual 2-D wake model based on Jensen wake model is adopted. As shown in Figure 10, the 2-D wake model takes partial wake effect into consideration according to the area-ratio principle, which is expected to estimate wind losses more accurately. Some scholars have also made similar modifications on Jensen wake model, such as Chowdhury, et al. [41], Wang, et al. [42], Amaral and Castro [43] and Hou, et al. [44].

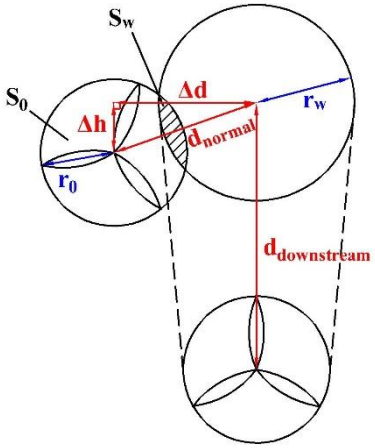

Figure 10 2-D wake model

In the 2-D wake model, the calculation of d_{normal} is different, and equation (9) should be adopted.

$$d_{normal} = \sqrt{\Delta h^2 + \Delta d^2} \tag{9}$$

The single wake equation is then modified as equation (10), whereas the multiple wake equation still adopts the equation (8).

$$\begin{cases} u = u_0, & r_w + r_0 < d_{normal} \\ u = u_0 \left[1 - \dfrac{2ar_0^2}{(r_0 + k \cdot d_{downstream})^2} \right] \cdot \dfrac{S_w}{S_0}, & r_w - r_0 \le d_{normal} \le r_0 + r_w \\ u = u_0 \left[1 - \dfrac{2ar_0^2}{(r_0 + k \cdot d_{downstream})^2} \right], & d_{normal} < r_w - r_0 \end{cases} \tag{10}$$

In the equations, r_0 is the blade radius of the WT; r_w is the radius of the wake-influenced area; s_0 is the swept area of the WT; and s_w is the wake-influenced area of the downstream WT. From equation (9), it is clear that the hub height difference is considered in the 2-D wake model. In the equation, Δh is the hub height difference between two WTs and Δd is the horizontal distance perpendicular to the downstream direction.

5. Case study

In this section, four cases are demonstrated and discussed. To verify the effectiveness of the Directional Restriction and the optimization method, the wind speeds assumed in the first three cases are smaller than the rated speeds for the WTs. If the wind speed is set larger than the rated speeds, 20 m/s for example, all WTs will generate energy as the rated power as long as they are installed meeting the qualifications of the restriction. It can be explained that the wind deficit caused by wake effect is limited, so the remaining wind speeds are still higher than the rated wind speeds of the WTs. Therefore, the proper setting of the incoming wind speed is really significant. In each case, the wind speed is identified. The potential wind farms in all cases are the square areas of 4 km by 4 km.

5.1 Case 1: aligned layout with uniform wind turbines

The first case is about an aligned arrangement of uniform WTs. The type of the WT is E-82, and the rated power is 2,000 kW. The number of WTs is 48, which means the capacity of the whole wind farm is 98.4 MW. To compare the performances of the two restrictions in the concentrated wind direction, a constant wind condition is adopted. The only direction of the wind is the north, and the wind speed at the hub height is 8.0 m/s, which is less than the rated wind speed 13 m/s.

When the Omnidirectional Restriction is adopted, the WTs are aligned with 6 rows and 8 columns, as shown in Figure 11. The minimum interval between WTs is longer than the 5D distance (410 m). Whereas, when the Directional Restriction is adopted, the WTs are aligned with 3 rows and 16 columns, as shown in Figure 12. The crosswind interval is shortened but larger than the 3D distance (246 m), and the downwind intervals increase correspondingly.

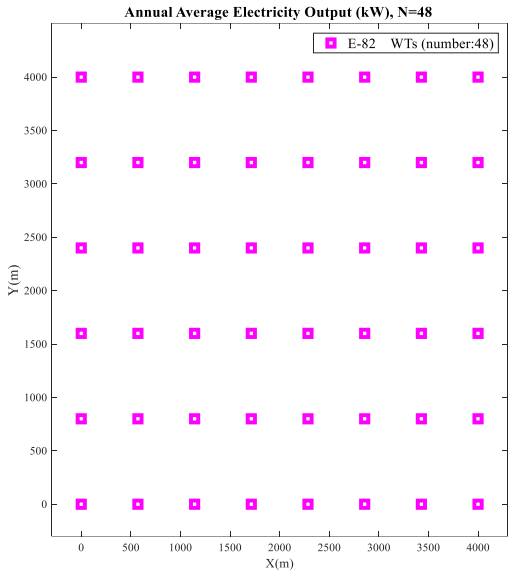

Figure 11 Aligned layout with the Omnidirectional Restriction

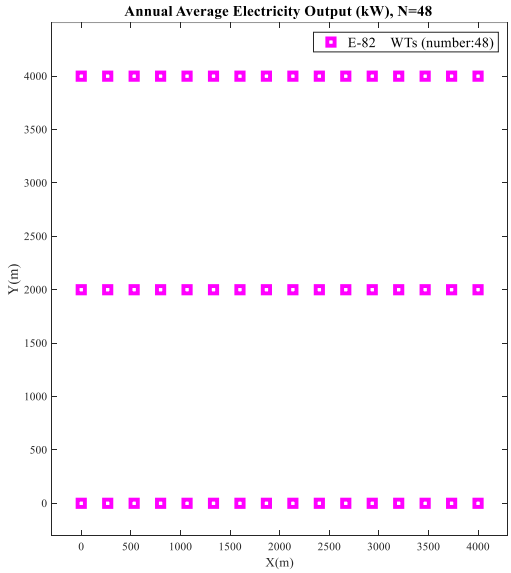

Figure 12 Aligned layout with the Directional Restriction

Table 2 lists the comparisons of the energy output of two restrictions. Theoretical output at given wind speed is also listed in the table. For E-82 WT, according to its power curve in Figure 5, the energy output is 837 kW at 8 m/s, which makes the total theoretical output as 40.18 MW.

Table 2 Comparisons of two types of restriction

Parameters	the Omnidirectional Restriction	the Directional Restriction
Number of wind turbine	48	48
Capacity (MW)	96.00	96.00
Theoretical output at given wind speed (MW)	40.18	40.18
Total Output (MW)	32.88	38.68
Utilization rate	81.83%	96.27%
The maximum wind turbine output (kW)	837	837
The minimum wind turbine output (kW)	650	787

To compare the effectiveness of different layouts, the utilization rate of wind farm is adopted, of which the formula is as follows:

$$\text{Utilization rate} = \frac{\text{Total output}}{\text{Theoretical output at given wind speed}} \times 100\% \quad (11)$$

From the results, the Directional Restriction has tremendous advantages under the circumstance of constant wind condition. When the type and the number of WTs are same, the layout with the Directional Restriction can avoid much more energy losses caused by the wake effect. The average power of the layout with Directional Restriction is 38.68 MW and the energy utilization ration is 96.27%, which are much more than the 32.88 MW output power and 81.83% utilization rate of the layout with the Omnidirectional Restriction. The increment of the utilization rate is 14.44%. The maximum WT outputs in both layouts are the same at 837 kW. The WTs with the maximum outputs are apparently those stand in the first line, facing the wind and not affected by any wakes. However, the situations of other WTs are much differing. The minimum WT output in the layout with the Directional Restriction is 787 kW, larger than that with the Omnidirectional Restriction (650 kW). This also attributes to the difference of the total energy outputs of two layouts. From the first case, it is indicated that the Directional Restriction is of practical use in aligned layout windfarm under the constant wind condition.

5.2 Case 2: optimized layout with uniform wind turbines

Case 2 then further investigated the optimization of the scattered arrangement. In this case, the type of WT, the total WT number and the wind condition are all the same as Case 1.

The optimization tool adopted in this study is the Multi-Population Genetic Algorithm (MPGA), which is widely used because of its high-efficiency merit. Gao, et al. [7], [45] have validated the effectiveness of applying the MPGA in the offshore wind farm optimization problem. The widely known procedure of the MPGA is shown in Figure 13. In the process of the MPGA, the first step is to define the objective function according to the problem to be solved and set a corresponding optimization criterion. In the second step, the initial population should be generated randomly. In the third step, the existing population should be taken into the function to evaluate the objective. The fourth step is to judge whether the optimization criterion is met. If the answer is yes, the best individuals are received. But if the optimization criterion is not met, the new population should be generated through the process of selection, recombination and mutation. Then the new population should go back into the circulation from the third step until the optimization criterion is met.

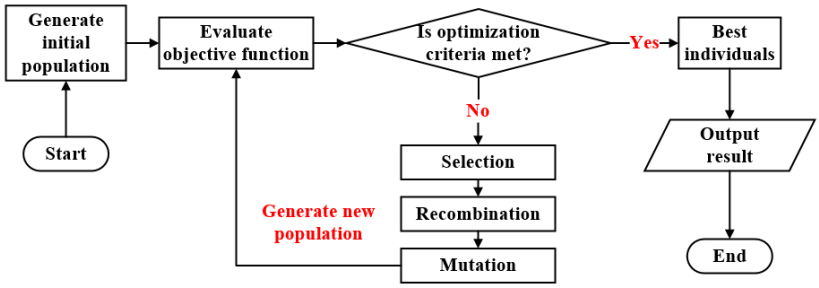

Figure 13 Procedure of the MPGA

In this case, the individual is the coordinate of the WT, which decides the layout of the wind farm. The total energy output is set as the objective and the optimization criterion is the judgment that whether the maximum total energy output keeps for 500 generations. If the criterion is satisfied, the optimal layout (i.e. the best individuals) is obtained; if not, the population will be selected, recombined and mutated until the criterion is satisfied. The number of WT is 48, which represents the number of individual in the optimization process is 48. The population is set as 10. The initial parameters setting for the MPGA in this case are listed in Table 3.

Table 3 The initial parameters setting for the MPGA in this study

Parameters	Values
Population number	10
Number of individuals	48
Binary digits of variable	20
Minimum generation	500
Probability of mutation	0.001-0.05
Probability of crossover	0.7-0.9

Figure 14 shows the optimized layout with the Omnidirectional Restriction, and Figure 15 shows the optimized layout with the Directional Restriction. The comparisons of the energy output of two restrictions are listed in Table 4.

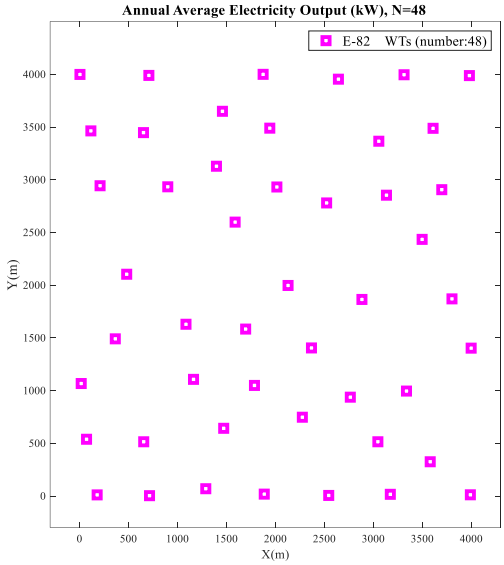

Figure 14 Optimized layout with the Omnidirectional Restriction

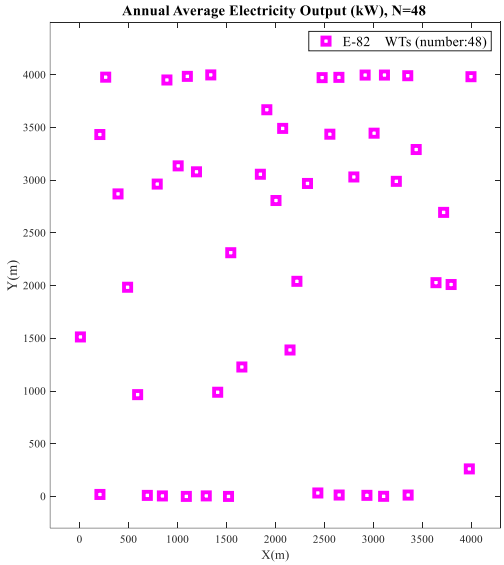

Figure 15 Optimized layout with the Directional Restriction

Table 4 Comparisons of two restrictions

Parameters	the Omnidirectional Restriction	the Directional Restriction
Number of wind turbine	48	48
Capacity (MW)	96.00	96.00
Theoretical output at given wind speed (MW)	40.18	40.18
Actual Output (MW)	39.35	39.72
Utilization rate	97.93%	98.86%
The maximum wind turbine output (kW)	837	837
The minimum wind turbine output (kW)	757	800

Case 2 not only demonstrates the comparison of two restrictions, but also verifies the effectiveness of the MPGA once again. Through the optimization process, the layout with the Omnidirectional Restriction improves the energy output compared to that of aligned layout in Case 1. To be specific, the increment of power output is from 32.88 MW to 39.35 MW, and the utilization rate increase by 16.10%, from 81.83% to 97.93%. As for the optimized layout with the Directional Restriction, it also raises the power output compared to the aligned layout, from 38.68 MW to 39.72 MW, with a utilization rate increase of 2.59% from 96.27% to 98.86%. The power output increment of the Directional Restriction is not prominent, just from 39.35 MW to 39.72 MW, and the utilization rate increase by 0.93%, from 97.93% to 98.86%, which is similarly not remarkable. This is because the efficiency of the original Directional Restriction is as high as 97.93%, so the room for improvement of utilization rate is really limited.

5.3 Case 3: optimized layout with nonuniform wind turbines

In this case, a nonuniform wind farm with multiple types of WTs is studied. The five adopted WTs are introduced in section 4.1. Total number of WT is 45 and the number of each type is 9, hence the capacity of the wind farm is 159.57 MW. The wind constantly blows from the north and the speed is 10.0 m/s at the hub height of 135 m. The MPGA is applied as the optimization tool. In this case, the Directional Restriction is applied, the restricted area of which is the 5D distance in downwind direction and the 2.5D distance in crosswind direction. Since diameters of WTs are different, the corresponding restricted areas are different as well.

It is well known that wind speed changes with height, therefore it is significant to know the wind speed at WT hub height [46, 47]. In this case, the wind speed variation with height is also taken into account. The wind power law is considered as a useful tool to describe the wind speed variation with height. It is used in this study, and the equation is as follows [48]:

$$v = v_0 \cdot \left(\frac{z}{z_0} \right)^{\alpha} \tag{12}$$

In the equation, z_0 is a reference height; v_0 is the known wind speed at z_0; v is the wind speed at height of z, and α is an empirically derived wind speed power law coefficient that varies dependent upon the stability of the atmosphere, the recommended value of α is shown in Table 5.

Table 5 Power exponent and gradient height for wind [7]

Terrain type	α	δ (m)
Lake, ocean and smooth hard ground	0.10	200
Open terrain with few obstacles (e.g. open grassland, shores, desert)	0.16	250
Terrain uniformly covered with obstacles 10–20 m (e.g. residential suburbs, woodland)	0.28	400
Terrain with large irregular objects (e.g. city centre, very broken country)	0.40	500

When wind blows through a considerable distance of from smooth terrain to rough terrain, equation (13) can describe the variation. V_g is the gradient wind velocity and remains unchanged:

$$V_1 = V_g \cdot \left(\frac{z_1}{\delta_1} \right)^{\alpha_1}, \quad V_2 = V_g \cdot \left(\frac{z_2}{\delta_2} \right)^{\alpha_2} \tag{13}$$

Consequently, the following equation can be obtained:

$$\frac{V_2}{V_1} = \left(\frac{z_2}{\delta_2} \right)^{\alpha_2} \cdot \left(\frac{\delta_1}{z_1} \right)^{\alpha_1} \tag{14}$$

Figure 16 demonstrates the final optimal layout. From the layout pattern, it is seen clearly that the restricted area is unique for each type of WT, especially in the crosswind direction.

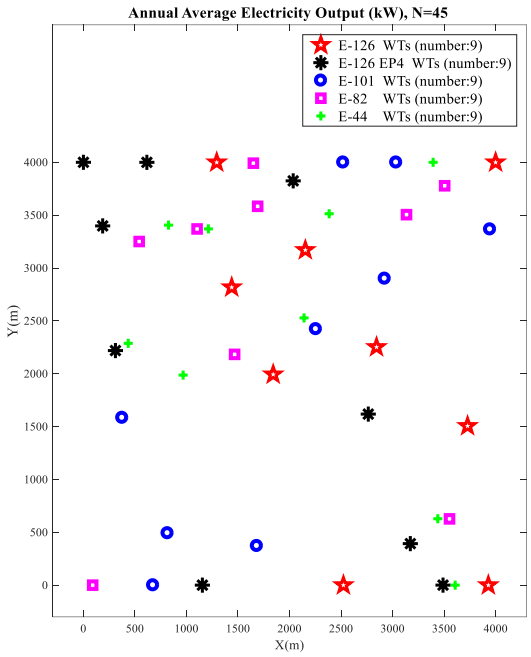

Figure 16 optimized layout with nonuniform wind turbines

The detailed analysis results of Case 3 are listed in Table 6. Since hub heights of WTs are different, the corresponding wind speeds at different hub heights are calculated and listed in the table. The maximum wind speed is 10.0 m/s at the height of 135 m, whereas the minimum one is 6.4 m/s at the height at 88 m. The theoretical outputs of each WTs are obtained from the wind power curves. The theoretical wind farm output is the sum of theoretical outputs of all WTs in the wind farm.

Table 6 Analysis of Case 3

Parameters	E-126 (7580 kW)	E-126 EP4 (4200 kW)	E-101 (3050 kW)	E-82 (2000 kW)	E-44 (900 kW)
Wind speed at hub height (m/s)	10.0	10.0	8.8	8.0	6.4
Theoretical single wind turbine output (kW)	3750	3097	1631	837	119
Number of wind turbine	9	9	9	9	9
The maximum wind turbine output (kW)	3750	3097	1631	837	119
Utilization rate of the maximum output	100%	100%	100%	100%	100%
The minimum wind turbine output (kW)	3596	3016	1564	789	117
Utilization rate of the minimum output	95.89%	97.38%	95.89%	94.27%	98.32%
Capacity (MW)			159.57		
Theoretical maximum wind farm output (MW)			84.91		
Optimized wind farm output (MW)			84.24		
Utilization rate of wind farm			99.21%		

From the table, the theoretical outputs of WTs are 3750 kW, 3097 kW, 1631 kW, 837 kW and 119 kW respectively. In wind farm, because of the wake effect, not every WT generates power as the predicted theoretical output. The maximum outputs and the minimum outputs of every type of WTs are also listed. Through the optimization process, the maximum outputs are all the same as the theoretical outputs, whereas the minimum outputs are 3596 kW, 3016 kW, 1564 kW, 789 kW and 117 kW respectively. Of all WTs in the wind farm, the minimum utilization rate is 94.27%, and the output of the wind farm is 84.24 MW, which makes the utilization rate as high as 99.21%. The effectiveness of the Directional Restriction and optimization method are further verified.

5.4 Case 4: a commercial nonuniform offshore wind farm

In this case, a real commercial wind farm is designed. Five types of WTs are used, the wind velocity is from the observation data, and the wind speed variation with height is also considered, which has been introduced in case 3. The MPGA is still the optimization tool and the Directional Restriction is also

applied, with the restriction of 5D distance in downwind direction and 3D distance in crosswind direction.

The potential wind farm site is chosen from Hong Kong sea areas. According to the study of Gao, et al. [7], four potential sea areas are suitable to build offshore wind farms in Hong Kong. Sha Chau Island sea area (as shown in Figure 17 and Figure 18) has a great potential of offshore wind resource and huge sea area to develop the offshore wind farm, so it is chosen in this case. The size of the selected offshore area is also 4 km×4 km.

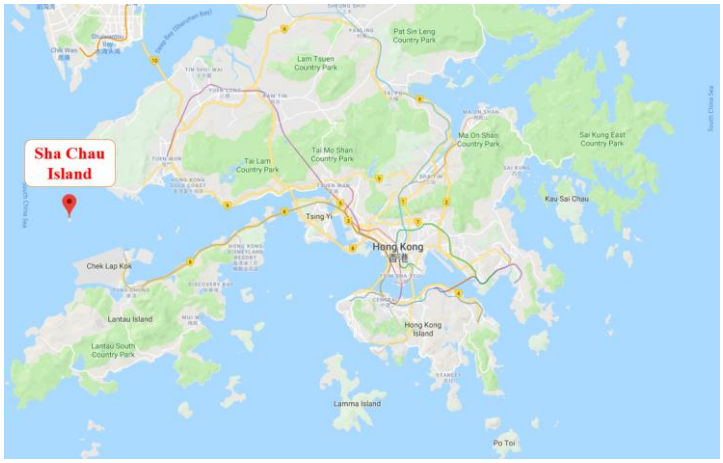

Figure 17 The location of Sha Chau Island [49]

Figure 18 Sha Chau Island [50]

The measured wind data of Sha Chau Island sea area is applied in this study. The first-hand wind data is the hourly wind speed data (from the years 2001 to 2011) comes from Royal Observatory, Hong Kong. The site of anemometer tower is 22°20'45" N, 113°53'28" E. The elevation of Sha Chau station is 21m above mean sea level, and the elevation of the anemometer is 31m above mean sea level. The hourly wind speed data are transferred into frequency distribution to be involved in the calculation process. The equation from hourly wind data to frequency distribution is seen as equation (15).

$$f(Dir, Spd) = \frac{N(Dir, Spd)}{N_{total}} \tag{15}$$

Then the 3-D wind velocity frequency distribution in Sha Chau Island sea area is shown in Figure 19.

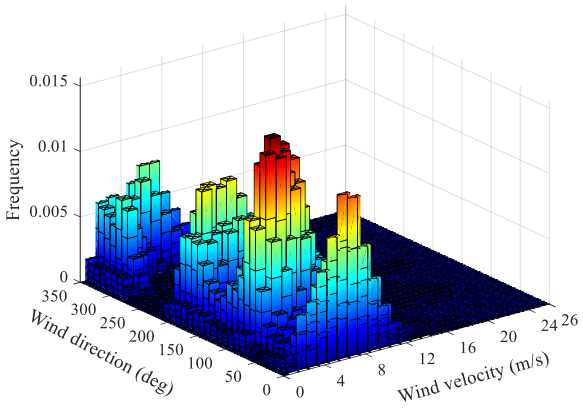

Figure 19 Wind velocity frequency distribution in Sha Chau Island sea area

From the 3-D distribution, it is directly perceived that the wind velocity in this area ranges from 0 m/s to 26 m/s, and mainly centers on around 7 m/s. The main wind direction centers on 100 ~ 140 , but also distributes on other directions. With the 3-D wind data distribution, the wind rose diagram and wind speed frequency distribution are obtained, as shown in Figure 20 and Figure 21. From the wind rose diagram, the wind direction is not centralized but distributed to three major directions.

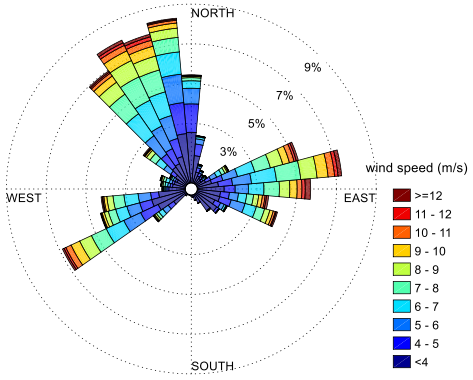

Figure 20 Wind rose diagram of Sha Chau

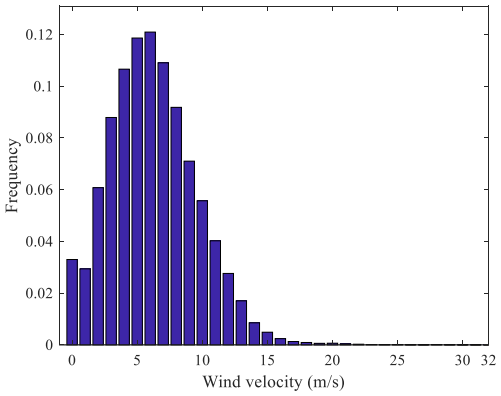

Figure 21 Wind speed frequency of Sha Chau

The wind farm is also designed with five types of WTs. The number of each type of the WT is 9, and the capacity of the wind farm is also 159.57 MW. Figure 22 demonstrates the final layout pattern of the optimized result. The directivity of the layout is not as obvious as the first three cases, this is because that the incoming wind direction is not highly-centralized.

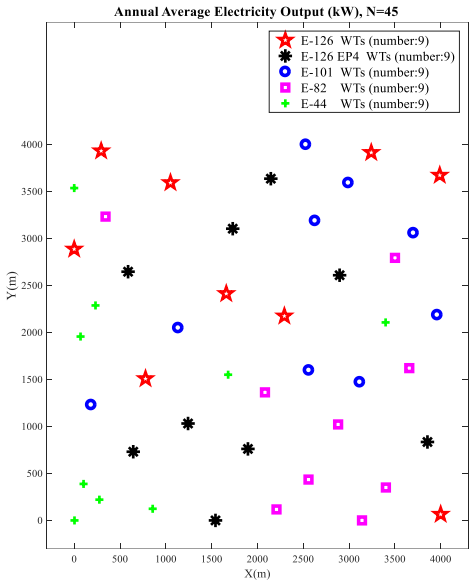

Figure 22 optimized layout of a commercial wind farm with nonuniform wind turbines

The analysis of Case 4 is listed in Table 7.

Table 7 Analysis of Case 4

Parameters	E-126 (7580 kW)	E-126 EP4 (4200 kW)	E-101 (3050 kW)	E-82 (2000 kW)	E-44 (900 kW)
Number of wind turbine	9	9	9	9	9
The maximum wind turbine output (kW)	4420	2822	2029	1304	481
The minimum wind turbine output (kW)	4335	2756	1990	1260	472
Capacity (MW)			159.57		
Optimized wind farm output (MW)			98.57		

With the Directional Restriction, this nonuniform offshore wind farm has the annual average power output of 98.57 MW. For the same type of WT, the differences between the maximum and the minimum power are very small. The maximum difference is only 85 kW from E-126 WTs. The average power output of WTs also demonstrates that the adopted optimization method is effective.

6. Conclusions

This paper conducted the research on the spacing restrictions of wind farms and the layout optimization problem of nonuniform wind farms. Comprehensive literature reviews were conducted. An original Directional Restriction was presented, which was applied in the optimization process of the nonuniform wind farm with various types of wind turbines. Four typical cases were studied to validate the presented Directional Restriction and the optimization method. Through this study, the main conclusions can be drawn:

(1) The presented Directional Restriction is effective for the wind farm where the direction of the prevailing wind is distinct. In the aligned layout design, where the wind direction was fixed and wind speed was constant, the Directional Restriction improved the energy utilization ration in a uniform wind farm by 14.44%. The similar increase in the optimized layout design was 0.93%.

(2) The Multi-Population Genetic Algorithm is a useful tool to solve the wind farm optimization problem. In the uniform wind farm, with the Omnidirectional Restriction, the optimization made an increase of 16.10% in energy utilization rate. The same increasing trend in the wind farm with the Directional Restriction was 2.59%.

(3) The nonuniform layout is effective in making use of the spatial wind source. In the nonuniform wind farm with five types of wind turbines, the optimization process with the Directional Restriction considered the wind speed variation with height. The utilization rate of the whole

wind farm was as high as 99.21%. The five maximum utilization rates of different types of wind turbines were all 100%, and the minimum utilization rate of all wind turbines was 94.27%.

(4) The Directional Restriction and the Multi-Population Genetic Algorithm were used in the layout optimization of a commercial nonuniform offshore wind farm. The potential site was chosen in Sha Chau Island seawater area in Hong Kong and the real measured wind data were adopted. The designed nonuniform offshore wind farm had an annual average power output of 98.57 MW. It demonstrated that the proposed optimization method is practical in designing wind farm, and Hong Kong offshore area is an ideal region to develop the offshore wind power.

Through this study, it is concluded that the optimization of the nonuniform wind farm using the Directional Restriction and the Multi-Population Genetic Algorithm is a practical method to make full use of wind resources. When applying the Directional Restriction, the wind condition will have a considerable influence on the layout of wind farm. If wind directions are highly-centralized, the optimal layout tends to be narrowly arrangement; while if wind directions are decentralized, the optimal layout may be scattered. In other words, for the region with highly-centralized wind directions, the Directional Restriction works more effectively. Meanwhile, the restricted area of the Directional Restriction tends to be smaller than that of the Omnidirectional Restriction. Therefore, the application of the Directional Restriction can also improve the capacity of wind farms by installing more wind turbines. To fully utilize the resources of wind farms and the benefits of the Directional Restriction, further study should be conducted on how to use the Directional Restriction to improve the capacity of the wind farm in a specific area. In addition, this is a theoretical study looking for ways to increase the utilization of wind energy in a given area, some aspects of building a real wind farm are neglected. Therefore, more problems such as cable layout, power transmission and economic cost should be further investigated in the near future.

Acknowledgement

The work described in this paper was supported by the Research Institute for Sustainable Urban Development (RISUD) with account number of BBW8, the FCE Dean Research project with account number of ZVHL, The Hong Kong Polytechnic University and National Natural Science Funds of China with grant number of 51606068.

References

[1] S. Mathew, *Wind energy : fundamentals, resource analysis and economics*. Berlin: Springer, 2006.

[2] Global Wind Energy Council, "Global wind 2017 report Annual Market Update," *Global Wind Energy Council (GWEC), Brussels, Belgium,* 2018.

[3] R. Perveen, N. Kishor, and S. R. Mohanty, "Off-shore wind farm development: Present status and challenges," *Renewable and Sustainable Energy Reviews,* vol. 29, pp. 780-792, 1// 2014.

[4] P. Hou, W. Hu, M. Soltani, and Z. Chen, "Optimized Placement of Wind Turbines in Large-Scale Offshore Wind Farm Using Particle Swarm Optimization Algorithm," *IEEE Transactions on Sustainable Energy,* vol. 6, no. 4, pp. 1272-1282, 2015.

[5] P. Hou, W. Hu, M. Soltani, B. Zhang, and Z. Chen, "Optimization of Decommission Strategy for Offshore Wind Farms," in *2016 IEEE Power & Energy Society General Meeting*, 2016.

[6] J. Twidell and G. Gaudiosi, *Offshore wind power*. Essex, United Kingdom: Multi Science Pub., 2009.

[7] X. Gao, H. Yang, and L. Lu, "Study on offshore wind power potential and wind farm optimization in Hong Kong," *Applied Energy,* vol. 130, pp. 519-531, 2014.

[8] "Hong Kong Energy End-use Data 2016," Electrical & Mechanical Services Department;2016.

[9] "Hong Kong Energy Statistics," Census and Statistics Department, Hong Kong Special Administrative Region2016.

[10] J. Feng and W. Z. Shen, "Design optimization of offshore wind farms with multiple types of wind turbines," *Applied Energy,* vol. 205, pp. 1283-1297, 2017/11/01/ 2017.

[11] G. Mosetti, C. Poloni, and B. Diviacco, "Optimization of wind turbine positioning in large windfarms by means of a genetic algorithm," *Journal of Wind Engineering and Industrial Aerodynamics,* vol. 51, no. 1, pp. 105-116, 1994.

[12] S. Grady, M. Hussaini, and M. M. Abdullah, "Placement of wind turbines using genetic algorithms," *Renewable energy,* vol. 30, no. 2, pp. 259-270, 2005.

[13] C. Zhang, G. Hou, and J. Wang, "A fast algorithm based on the submodular property for

optimization of wind turbine positioning," *Renewable Energy,* vol. 36, no. 11, pp. 2951-2958, 2011/11/01/ 2011.
[14] J. Park and K. H. Law, "Layout optimization for maximizing wind farm power production using sequential convex programming," *Applied Energy,* vol. 151, pp. 320-334, 8/1/ 2015.
[15] P. Mittal, K. Kulkarni, and K. Mitra, "A novel hybrid optimization methodology to optimize the total number and placement of wind turbines," *Renewable Energy,* vol. 86, pp. 133-147, Feb 2016.
[16] L. Parada, C. Herrera, P. Flores, and V. Parada, "Wind farm layout optimization using a Gaussian-based wake model," *Renewable Energy,* vol. 107, pp. 531-541, Jul 2017.
[17] Wikipedia. *Tehachapi Pass Wind Farm*. Available: https://en.wikipedia.org/wiki/Tehachapi_Pass_Wind_Farm
[18] J.-F. Herbert-Acero, J.-R. Franco-Acevedo, M. Valenzuela-Rendón, and O. Probst-Oleszewski, "Linear wind farm layout optimization through computational intelligence," in *Mexican International Conference on Artificial Intelligence*, 2009, pp. 692-703: Springer.
[19] S. Annealing and B. Machines, "A Stochastic Approach to Combinatorial Optimization and Neural Computing," ed: Chichester (Wiley), 1991.
[20] D. Hand, "Genetic algorithms in search, optimization and machine learning," *Statistics and Computing,* vol. 4, no. 2, p. 158, 1994.
[21] Y. Chen, H. Li, K. Jin, and Q. Song, "Wind farm layout optimization using genetic algorithm with different hub height wind turbines," *Energy Conversion and Management,* vol. 70, pp. 56-65, 2013/06/01/ 2013.
[22] S. Chowdhury, J. Zhang, A. Messac, and L. Castillo, "Optimizing the arrangement and the selection of turbines for wind farms subject to varying wind conditions," *Renewable Energy,* vol. 52, pp. 273-282, 2013/04/01/ 2013.
[23] K. Chen, M. X. Song, and X. Zhang, "The iteration method for tower height matching in wind farm design," *Journal of Wind Engineering and Industrial Aerodynamics,* vol. 132, pp. 37-48, 2014/09/01/ 2014.
[24] K. Chen, M. X. Song, X. Zhang, and S. F. Wang, "Wind turbine layout optimization with multiple hub height wind turbines using greedy algorithm," *Renewable Energy,* vol. 96, pp. 676-686, 2016/10/01/ 2016.
[25] J. Lee, D. R. Kim, and K.-S. Lee, "Optimum hub height of a wind turbine for maximizing annual net profit," *Energy Conversion and Management,* vol. 100, pp. 90-96, 2015/08/01/ 2015.
[26] A. Vasel-Be-Hagh and C. L. Archer, "Wind farm hub height optimization," *Applied Energy,* vol. 195, pp. 905-921, 2017/06/01/ 2017.
[27] M. Song, K. Chen, and J. Wang, "Three-dimensional wind turbine positioning using Gaussian particle swarm optimization with differential evolution," *Journal of Wind Engineering and Industrial Aerodynamics,* vol. 172, pp. 317-324, 1// 2018.
[28] ENERCON GmbH. ENERCON product overview [Online]. Available: https://www.enercon.de/fileadmin/Redakteur/Medien-Portal/broschueren/pdf/en/ENERCON_Produkt_en_06_2015.pdf
[29] Z. Song, Z. Zhang, and X. Chen, "The decision model of 3-dimensional wind farm layout design," *Renewable Energy,* vol. 85, pp. 248-258, 1// 2016.
[30] R. J. Barthelmie *et al.*, "Modelling and measuring flow and wind turbine wakes in large wind farms offshore," *Wind Energy,* vol. 12, no. 5, pp. 431-444, 2009.
[31] B. Sanderse, "Aerodynamics of wind turbine wakes," *Energy Research Center of the Netherlands (ECN), ECN-E–09-016, Petten, The Netherlands, Tech. Rep,* 2009.
[32] M. L. Thogersen, T. Sorensen, P. Nielsen, A. Grotzner, and S. Chun, "Introduction to wind turbine wake modelling and wake generated turbulence," *DNV/Risø, 2nd ed.: Risø National Laboratory, EMD International A/S,* 2006.
[33] Y.-K. Wu, C.-Y. Lee, C.-R. Chen, K.-W. Hsu, and H.-T. Tseng, "Optimization of the Wind Turbine Layout and Transmission System Planning for a Large-Scale Offshore WindFarm by AI Technology," *IEEE Transactions on Industry Applications,* vol. 50, no. 3, pp. 2071-2080, 2014.
[34] A. Kusiak and H. Zheng, "Optimization of wind turbine energy and power factor with an evolutionary computation algorithm," *Energy,* vol. 35, no. 3, pp. 1324-1332, 2010.
[35] Y. Eroğlu and S. U. Seçkiner, "Design of wind farm layout using ant colony algorithm," *Renewable Energy,* vol. 44, pp. 53-62, 2012.
[36] B. Pérez, R. Mínguez, and R. Guanche, "Offshore wind farm layout optimization using mathematical programming techniques," *Renewable Energy,* vol. 53, pp. 389-399, 2013.

[37] S. Pookpunt and W. Ongsakul, "Optimal placement of wind turbines within wind farm using binary particle swarm optimization with time-varying acceleration coefficients," *Renewable Energy,* vol. 55, pp. 266-276, 2013.
[38] N. O. Jensen, *A note on wind generator interaction*. 1983.
[39] R. Shakoor, M. Y. Hassan, A. Raheem, and Y.-K. Wu, "Wake effect modeling: A review of wind farm layout optimization using Jensen′s model," *Renewable and Sustainable Energy Reviews,* vol. 58, pp. 1048-1059, 5// 2016.
[40] H. Sun and H. Yang, "Study on an innovative three-dimensional wind turbine wake model," *Applied Energy,* vol. 226, pp. 483-493, 2018/09/15/ 2018.
[41] S. Chowdhury, J. Zhang, A. Messac, and L. Castillo, "Unrestricted wind farm layout optimization (UWFLO): Investigating key factors influencing the maximum power generation," *Renewable Energy,* vol. 38, no. 1, pp. 16-30, 2012.
[42] L. Wang, A. C. C. Tan, M. Cholette, and Y. Gu, "Comparison of the effectiveness of analytical wake models for wind farm with constant and variable hub heights," *Energy Conversion and Management,* vol. 124, pp. 189-202, 2016/09/15/ 2016.
[43] L. Amaral and R. Castro, "Offshore wind farm layout optimization regarding wake effects and electrical losses," *Engineering Applications of Artificial Intelligence,* vol. 60, pp. 26-34, 4// 2017.
[44] P. Hou, P. Enevoldsen, W. Hu, C. Chen, and Z. Chen, "Offshore wind farm repowering optimization," *Applied Energy,* vol. 208, pp. 834-844, 2017.
[45] X. Gao, H. Yang, and L. Lu, "Investigation into the optimal wind turbine layout patterns for a Hong Kong offshore wind farm," *Energy,* vol. 73, pp. 430-442, 2014.
[46] G. L. Johnson, *Wind energy systems*. Prentice-Hall Englewood Cliffs (NJ), 1985.
[47] A. Ilinca, E. McCarthy, J.-L. Chaumel, and J.-L. Rétiveau, "Wind potential assessment of Quebec Province," *Renewable energy,* vol. 28, no. 12, pp. 1881-1897, 2003.
[48] Wikipedia. *Wind profile power law*. Available: https://en.wikipedia.org/wiki/Wind_profile_power_law
[49] Google Map, "Sha Chau Island," ed, 2018.
[50] Wikipedia. *Sha Chau*. Available: https://en.wikipedia.org/wiki/Sha_Chau